Preprints of the 2012 20th Mediterranean Conference on Control & Automation (MED), Barcelona, Spain, July 3-6, 2012

Study on Residual Vibration Suppression for a Flexible Dual-Manipulator

Akira Abe and Kohei Yoshida

Abstract— **This paper presents a feedforward control technique for suppressing residual vibrations of a flexible dual-manipulator. To construct the mathematical model of the manipulator system accurately, the parameters of the equations of motion are experimentally identified. In the control technique, we express the joint angle by a cubic spline function, and then use a particle swarm optimization to find an optimal path. The optimal path thus obtained carries a minimum vibration requirement. The suppression of the residual vibrations of the flexible dual-manipulator can be accomplished by rotating the joint angle along the optimal path. The validity and effectiveness of the proposed vibration control scheme is substantiated by simulation and experimental results.**

I. Introduction

When lightweight manipulators perform a high-speed pick and place operation, unwanted vibrations may occur because of their flexibility. How to suppress these unwanted vibrations of flexible robotic manipulators is a significant problem, and therefore a considerable number of research regarding vibration control problems are available. Benosman and Vey [1] published an exhaustive literature review on various vibration control techniques applicable to flexible manipulators. Dwivedy and Eberhard [2] also compiled a comprehensive list of publications (up to 2005), dealing with the dynamic analysis and control of flexible manipulators.

Vibration control schemes can be broadly classified into two categories: feedforward and feedback. The advantage of feedforward control schemes is that the control systems can be manufactured at low cost because they do not require vibration-measuring sensors.

With regard to feedforward control, Yue et al. [3] developed a trajectory planning method to minimize the vibration and/or execution time of a point-to-point (PTP) motion for flexible redundant robot manipulators based on genetic algorithms. Lee and Park [4] proposed a modified input shaping method to reduce the vibration of a two-link flexible manipulator after a rest-to-rest motion. To significantly reduce the residual vibration of flexible manipulators in the presence of obstacles [5] and under torque constraints [6], Park proposed optimal path design techniques based on a combined Fourier series and polynomial. A feedforward vibration control scheme for a flexible robot manipulator system using input shaping and filtering techniques was developed by Mohamed and Tokhi [7]. Feliu et al. [8] investigated a method that combines feedforward control with an optimal mechanical design to cancel vibrations in a multimode single-link flexible manipulator. An evolutionary learning acquisition method on residual vibration reduction of a flexible robot arm consisting of a first rigid link and a second flexible link was proposed by Kojima and Hiruma [9]. Alam and Tokhi [10] applied a multi-objective genetic algorithm to design command-shaping techniques and achieved vibration control of a single-link flexible manipulator. Díaz et al. [11] dealt with active vibration cancellation in flexible manipulators. They developed a novel concurrent design of a robust multimode input shaper and a modification of the link dynamics. The present authors proposed residual vibration suppression techniques for a two-link rigid-flexible manipulator [12] and a flexible Cartesian robot manipulator [13] with a PTP motion. In the techniques, a particle swarm optimization (PSO) algorithm (e.g., [14], [15]) was utilized to generate the optimal trajectory satisfying the minimum residual vibration requirements. However, there exist only a few reports dealing with a flexible dual-arm robot [16], in which two flexible links are attached to one vehicle. In [16], an optimal trajectory planning method for vibration reduction during a robot motion was presented.

This paper proposes a novel method for the trajectory planning of two flexible manipulators attached to one motor hub to suppress residual vibrations in a PTP motion. Unlike the previous works of [12] and [13], we attempt here to develop a feedforward technique for a system with two vibration modes. The equations of motion for the manipulator system, which are nonlinear differential equations, are developed using the Lagrangian approach and the assumed modes method. To construct the mathematical model accurately, the coefficients of the obtained equations are identified by an experiment. In the trajectory planning, the profile of the joint angle of the two flexible links is expressed using a cubic spline function, and then the interpolation points satisfying the minimum residual vibration requirement are tuned using a PSO. The suppression of the residual vibrations of the two flexible links can be accomplished by rotating the joint along the generated trajectory, that is, the proposed control scheme is a feedforward control that does not require sensors to measure unwanted vibrations. The application of an input shaper (e.g., [7], [10]), which is one of widely used feedforward controllers, is restricted to linear systems. On the other hand, the proposed method

This work was in part supported by the Japan Society for the Promotion of Science (JSPS) KAKENHI, Grant-in-Aid for Scientific Research (C), 23560274.

A. Abe is with the Department of Systems, Information and Control Engineering, Asahikawa National College of Technology, Asahikawa, Hokkaido 071-8142, Japan abe@asahikawa-nct.ac.jp

K. Yoshida is with the Department of Information System Engineering, Asahikawa National College of Technology, Asahikawa, Hokkaido 071-8142, Japan.

978-1-4673-2529-5/12/$31.00 ©2012 IEEE

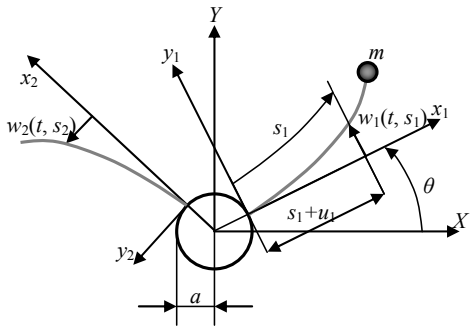

Fig. 1. Schematic of a flexible dual-manipulator system.

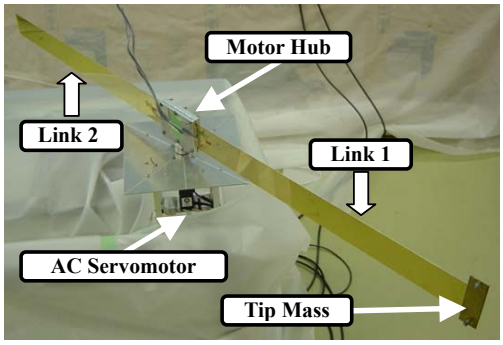

Fig. 2. Photograph of the experimental setup.

has the advantage of being applicable to nonlinear systems. Numerical simulation results demonstrate the effectiveness of the proposed vibration control scheme for the suppression of residual vibrations. Furthermore, the validity of the proposed method is also experimentally confirmed.

II. Mathematical Modeling

Fig. 1 shows the schematic of a flexible dual-manipulator system, in which two flexible links are attached to one motor hub. Here, a is the radius of the rigid hub, θ is the joint angle, and w_i and u_i are the transverse and axial displacements of the flexible link i ($i = 1,2$), respectively. Noted that u_i represents the effects of geometric nonlinearities arising from large transverse deformation [12], and is given by

$$u_i = -\frac{1}{2}\int_0^{s_i}\left(\frac{\partial w_i}{\partial s_i}\right)^2 ds_i, \quad (i = 1,2), \tag{1}$$

where s_i is the coordinate along the deformed configuration of the flexible link i. Since the two flexible links are constrained to move only in the horizontal plane, the influence of gravity on the movement of the system is negligible.

According to the Euler–Bernoulli theory, the system's kinetic and potential energies T and U can be represented as

$$T = \frac{1}{2}\left(J\dot{\theta}^2 + \sum_{i=1}^{2}\rho_i A_i\int_0^{l_i}\dot{\boldsymbol{r}}_i^{\mathrm{T}}\dot{\boldsymbol{r}}_i ds_i + m\dot{\boldsymbol{r}}_1^{\mathrm{T}}\dot{\boldsymbol{r}}_1|_{s_1=l_1}\right), \tag{2}$$

$$U = \frac{1}{2}\sum_{i=1}^{2}E_i I_i\int_0^{l_i}\left(\frac{\partial^2 w_i}{\partial s_i^2}\right)^2 ds_i, \tag{3}$$

where J is the hub inertia and m is the tip mass of the flexible link 1. The density, cross-sectional area, length, and flexural rigidity of the flexible link i are denoted by ρ_i, A_i, l_i, and E_iI_i, respectively. The position vector $\boldsymbol{r}_i$ of the flexible link i relative to the inertial frame (X,Y) at an arbitrary location s_i can be expressed as

$$\boldsymbol{r}_i = \begin{bmatrix} (a+s_i+u_i)\cos\vartheta_i - w_i\sin\vartheta_i \\ (a+s_i+u_i)\sin\vartheta_i + w_i\cos\vartheta_i \end{bmatrix}. \tag{4}$$

The angle ϑ_i is defined as

$$\vartheta_1 = \theta, \quad \vartheta_2 = \theta + \gamma, \tag{5}$$

where γ is the angle between the x_1 and x_2 axes.

It is assumed that the motions of the two flexible links are dominated by the first vibration mode, and that the displacements of the higher vibration modes are negligible. This assumption is justified by experimental results. According to the assumed mode method, the transverse displacements of the flexible links can be expressed using the eigenfunction $\phi_i(s_i)$ of the first vibration mode as

$$w_i(t,s_i) = W_i(t)\phi_i(s_i), \tag{6}$$

where $W_i(t)$ is a time function. The equations of motion for the two flexible links can be obtained from the Lagrangian approach, which is represented as follows.

$$\frac{d}{dt}\left(\frac{\partial L}{\partial \dot{W}_i}\right) - \frac{\partial L}{\partial W_i} = 0, \tag{7}$$

where $L = T - U$. Substituting (6) into (2) and (3) and taking the partial derivatives in (7), we obtain the following equations.

$$\begin{aligned}(1+2\beta_{2i}W_i^2)\ddot{W}_i + 2\zeta_i\omega_i\dot{W}_i + \omega_i^2 W_i + (\alpha_i+\beta_{3i}W_i^2)\ddot{\theta} \\ + 2\beta_{4i}\dot{W}_i^2 W_i + (\beta_{1i}-\beta_{5i}W_i^2)W_i\dot{\theta}^2 = 0, \ (i=1,2),\end{aligned} \tag{8}$$

where ω_i is the natural frequency, and α_i and β_{ji} are the coefficients of the linear and nonlinear terms, respectively. The damping coefficient ζ_i is introduced because of the experimental setup. It is noted that the values of the coefficients α_i and β_{ji} are not dependent upon the angle γ. In this study, we assume that the tracking control of the joint angle can be realized. Under this assumption, the rigid body motion of the links can be neglected [12], [13]. Therefore, only (8), which expresses the dynamics of the flexible links, is used in the present study.

III. Experimental Setup and Parameter Identification

A. Experimental Setup

An overview of the experimental setup is shown in Fig. 2. Two flexible links, which are made of a brass beam of length $l = 550$ mm, width $b = 50$ mm, and thickness $h = 0.8$ mm, are attached to a motor hub. The size of the two flexible links is the same, while a mass of the weight $m = 36$ g, is attached to the endpoint of the flexible link 1. Fig. 3 depicts a schematic of the experimental setup.

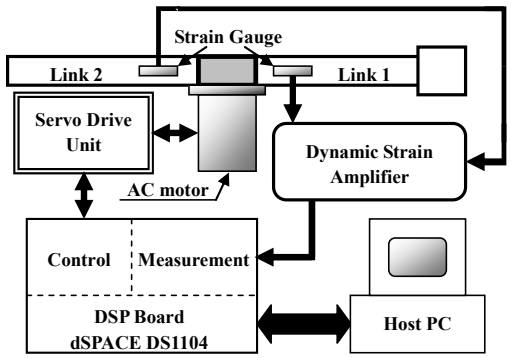

Fig. 3. Schematic of the experimental setup.

As shown in Figs. 2 and 3, an AC servomotor (Yaskawa Electric Co.: SGMMJ–A3EAAJ361K) is employed as the actuator. The servomotor is driven by a servo drive unit (Yasukawa Electric Co.: DGDV–A3ESY32). In this case, the servomotor can be operated in the speed control mode. The joint angle is measured by a serial encoder mounted on the servomotor. A strain gauge is attached on one side to measure the deflection of the flexible links. The signals from the strain gauges are amplified with a dynamic strain amplifier (Tokyo Sokki Kenkyujo Co.: DA–36A). The monitor and control of the experimental setup are implemented on a DSP board (dSPACE: DS1104), which has a sampling rate of 500 Hz.

B. Parameter Identification Technique

The proposed method for residual vibration suppression belongs to a group of feedforward control techniques that generally require exact mathematical models. Thus, in order to construct the mathematical model accurately, the parameters of the obtained equations are first identified experimentally.

First, in the identification experiment [13], the joint angle is rotated along a cycloidal motion path

$$\theta_{cyc}(t) = \theta_E \left[\frac{t}{T_E} - \frac{1}{2\pi} \sin\left(\frac{2\pi t}{T_E} \right) \right], \quad (0 \le t \le T_E), \quad (9)$$

and then the displacements of the flexible links are measured for 3 s. Here, the traveling time T_E and the target angle θ_E are set to 1 s and $\pi/2$ rad, respectively. To track a given reference angle θ_{ref}, the input voltage supplied to the servo drive unit v is given as

$$v = v_{ref} + K_1(\theta_{ref} - \theta) + K_2(\dot{\theta}_{ref} - \dot{\theta}), \quad (10)$$

where v_{ref} is the reference voltage corresponding to $\dot{\theta}_{ref}(t)$ in the speed control mode, and K_1 and K_2 are feedback gains of the PD control. The feedback gains are set to $K_1 = 20$ and $K_2 = 0.1$, which are determined by trial and error.

Next, we attempt to equalize the displacements obtained by the numerical integration of (8) and those obtained by the above experiment. For this purpose, an objective function is defined as follows.

$$f_i = \sum_{k=1}^{K} |W_{eik} - W_{sik}|, \quad (11)$$

TABLE I
IDENTIFIED PARAMETERS

Parameter	Link 1	Link 2
ω [rad/s]	7.961	10.37
ζ [–]	9.671×10^{-3}	1.967×10^{-3}
α [kgm^2]	3.899×10^{-1}	2.389×10^{-1}
β_1 [–]	3.583×10^{-3}	3.020×10^{-3}

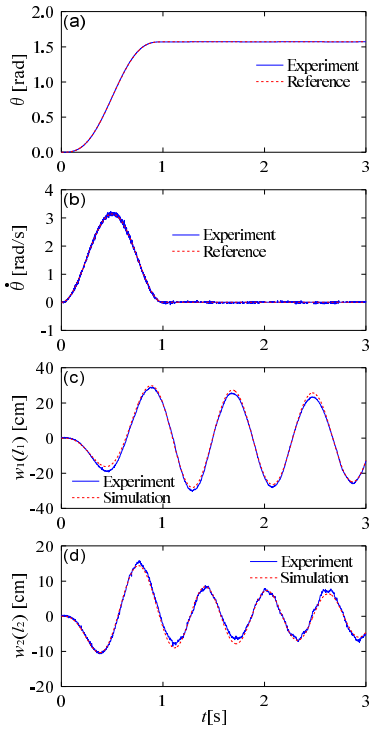

Fig. 4. Identified results ($T_E = 1.0$ s, $\theta_E = \pi/2$ rad): (a) joint angle, (b) angular velocity, (c) tip displacement of flexible link 1, and (d) tip displacement of flexible link 2.

where W_{eik} and W_{sik} are the experimental and simulation results, respectively, for each of the flexible links at the sampling time $\Delta t = 2$ ms. To minimize the objective function as much as possible, the parameters of (8) are tuned by the PSO algorithm developed by Clerc and Kennedy [15]. Finally, the PSO tuning method for the parameters ω_i, α_i, β_{ji}, and ζ_i yields the accurate models of the flexible links.

Table I lists the values of the identified parameters. Noted that the parameters β_{2i}–β_{5i} are negligible (i.e., the values are equal to zero) because the effect of those parameters on the dynamics of the flexible links is very small.

The identification results are presented in Fig. 4. The joint angle and angular velocity are displayed in Figs. 4(a) and (b), respectively. From these figures, it can be seen that the experimental results (solid line) are in fair agreement with the reference values (dotted line). Therefore, we can confirm that the control law (10) is valid for tracking the joint angle. A comparison of the simulation and experimental results of the tip displacements is given in Figs. 4(c) and (d). These

figures show that the tip displacements of the two flexible links obtained from the simulation and experimental results are in reasonable agreement with each other. Consequently, we can say that the identification results of the parameters in (8) are accurate.

On the other hand, we observe in Figs. 4(c) and (d) that residual vibrations (i.e., the displacements after positioning) occur when the dual-manipulator system is driven along the cycloidal motion. In the next section, we will present a trajectory planning method for suppressing the residual vibrations.

IV. Optimal Trajectory Planning for Residual Vibration Suppression

In this study, we consider a PTP motion of a flexible dual-manipulator for a fixed traveling time T_E and target angle θ_E. To suppress the residual vibrations of the two flexible links, we developed an optimal trajectory planning method for the joint angle by using a cubic spline function.

The concept of the proposed method can be illustrated using the scheme shown in Fig. 5. We divide the travelling time T_E into $2N$ divisions and define the discrete joint angle θ_n. Noted that θ_{10} denotes θ_E. To generate the trajectory of the joint angle $\theta(t)$, a cubic spline, which is defined as a set of polynomial functions, is used to interpolate the discrete angles. The joint angular velocity $\dot{\theta}(t)$ and acceleration $\ddot{\theta}(t)$ are obtained by differentiating the spline curves with respect to time. In the present study, the discrete angles are defined by introducing parameters $\Delta\theta_n$ as follows.

$$\left.\begin{aligned} &\theta_{n+1} = \theta_{cyc}(t_{n+1}) + \Delta\theta_n, \quad (n = 1,2,\cdots,N-1) \\ &\theta_{2N-1-n} = \theta_E - \theta_{n+1}, \quad (n = 1,2,\cdots,N-2) \end{aligned}\right\}. \quad (12)$$

As shown in (12) and Fig. 5, the parameters $\Delta\theta_n$ represent the deviation from the trajectory for the cycloidal motion (9). In the cubic spline interpolation, we employ the following initial and final conditions.

$$\theta(0) = 0, \quad \theta(T_E) = \theta_E, \quad \dot{\theta}(0) = \dot{\theta}(T_E) = 0. \quad (13)$$

To realize a smooth motion, it is desirable that not only the velocity but also the acceleration of the joint angle be equal to zero at the start and end points of the PTP motion. In the present study, the discrete joint angles θ_1 and θ_{2N-1} are determined such that they satisfy the condition $\ddot{\theta}(0) = \ddot{\theta}(T_E) = 0$. Consequently, the abovementioned technique enables the trajectory $\theta(t)$ to be expressed in terms of the parameters $\Delta\theta_n$, whose number is only $N-1$ for the $2N$ divisions of T_E.

The proposed trajectory planning method, which is a feedforward controller for the two flexible links, can be summarized as follows. The angular velocity $\dot{\theta}(t)$ and acceleration $\ddot{\theta}(t)$ are obtained from the differentiation of the joint angle $\theta(t)$. Next, the numerical integration of (8) yields the displacements $W_i(t)$. Aiming to minimize the residual vibrations of the two flexible links simultaneously, we define an objective function as follows.

$$F = \max_{t\in S}\left[|w_1(t,l_1)| + |w_2(t,l_2)|\right], \ (S: T_E \le t \le T_E + 1), \quad (14)$$

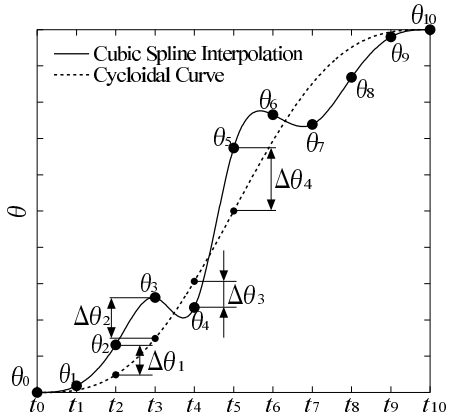

Fig. 5. Schematic of trajectory planning ($N = 5$)

where F indicates the maximum value of the sum of the two displacements at 1 s after the positioning. The parameters $\Delta\theta_n$ $(n = 1,2,\cdots,N-1)$ are considered to be optimized, and the minimization of the objective function (14) is carried out using the PSO. Finally, this algorithm generates the optimal trajectory of the joint angle for the residual vibration suppression.

V. Results and Discussion

To verify the performance of the proposed trajectory planning method described in Section IV, some simulation and experimental results are presented in this section.

A. Simulation Results

In the following numerical simulations, the PSO used 50 particles and a maximum of 200 iterations. The search space of the optimized parameters is taken to be

$$\Delta\theta_n \in [-\theta_{cyc}(t_{n+1})/3, \ \theta_{cyc}(t_{n+1})/3], \quad (n = 1,2,\cdots,N-1). \quad (15)$$

The number of trajectory partitions N is set to 5. The ranges of the search space and the number of the partitions are determined by trial and error.

First, we consider the PTP motion in which the traveling time and target angle are the same as in Fig. 4. Fig. 6 is a comparison of the simulation results obtained by the present method and the cycloidal motion. In the figures, the solid and dotted lines denote the present method and the cycloidal motion, respectively. From Figs. 6(c) and (d), it can be seen that the residual vibrations of the two flexible links are completely suppressed by using the present approach. When the joint angle is rotated along the trajectory of the cycloidal motion, the amplitudes of the residual vibrations of links 1 and 2 are approximately 28 and 8 cm, respectively. Therefore, it can be said that the proposed trajectory planning method is quite effective for residual vibration suppression.

To further evaluate the efficacy of the trajectory planning method, we change the traveling time T_E and target angle θ_E. Fig. 7 shows the simulation results under the conditions $T_E =$

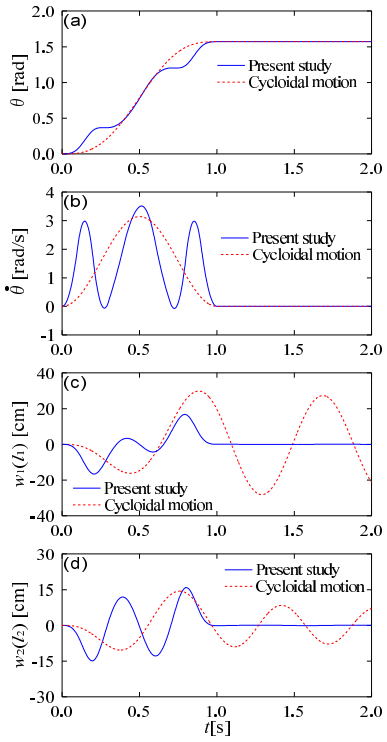

Fig. 6. Comparison of simulation results obtained by the present method and cycloidal motion ($T_E = 1.0$ s, $\theta_E = \pi/2$ rad): (a) joint angle, (b) angular velocity, (c) tip displacement of flexible link 1, and (d) tip displacement of flexible link 2.

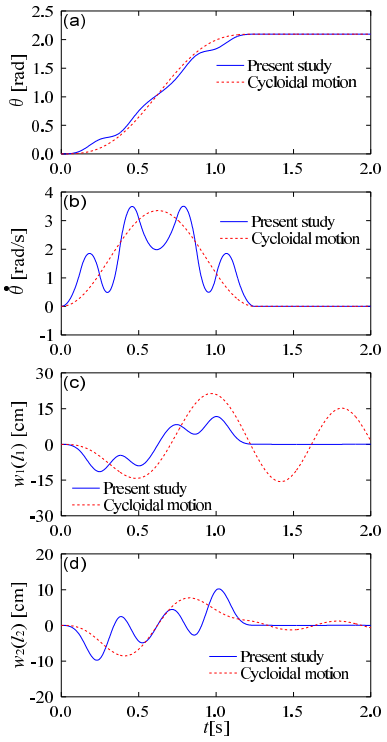

Fig. 7. Comparison of simulation results obtained by the present method and cycloidal motion ($T_E = 1.25$ s, $\theta_E = 2\pi/3$ rad): (a) joint angle, (b) angular velocity, (c) tip displacement of flexible link 1, and (d) tip displacement of flexible link 2.

1.25 s and $\theta_E = 2\pi/3$ rad. In the case of cycloidal motion, it can be determined from Fig. 7(d) that the residual vibration amplitude of the flexible link 2 is relatively smaller than that in Fig. 6 (d) The reason is that the travelling time is nearly twice the natural period. As can be seen from Figs. 7(c) and (d), the simultaneous cancelation of the residual vibrations again takes place, which reconfirms the effectiveness of the proposed method.

B. Experimental Results

From the simulation results, it is clear that the trajectory planning method can perfectly eliminate the residual vibrations of the two flexible manipulators attached to one motor hub. To consolidate the validity of the proposed vibration control technique, we carry out the following experiment.

Figs. 8 and 9 illustrate the experimental results under the conditions used in Figs. 6 and 7, respectively. In these figures, the results obtained from the present method (solid line) and the cycloidal motion (dotted line) are compared. If residual vibrations occur when the manipulator is operating along the cycloidal motion trajectory, the vibrations after the positioning are canceled using the present approach. In the experimental setup, the vibration controls are realized by driving the joint angle along the optimal path. Thus, we can conclude that the proposed feedforward control technique is valid and effective for suppressing the residual vibrations. The fact that the residual vibrations are suppressed in the experiment also demonstrates the effectiveness of the identification technique and tracking control presented in Section III.

On the other hand, as can be observed from the experimental responses shown in Figs. 8(c), 8(d), 9(c) and 9(d), the present method is not influenced by the higher vibration modes. This proves that the higher modes are not activated when the manipulator is rotated along the trajectory obtained through the cubic spline function whose interpolation points are tuned by the PSO. Therefore, we can say that the assumption adopted for the mathematical modeling in Section II is valid and the present method generates a smooth motion.

VI. Conclusion

In this study, we dealt with a PTP motion task of two flexible manipulators attached to one motor hub, and presented an optimal trajectory planning technique for suppressing residual vibrations of the flexible links. A cubic spline function was utilized to generate the optimal trajectory of the joint angle. To suppress residual vibrations of the two flexible links simultaneously, the maximum value of the sum of the two displacements after positioning was defined as an objective function. A PSO was employed to minimize the objective function, and then the optimal trajectory satisfying the minimum vibration condition was obtained. Numerical simulations revealed that when the joint angle was driven

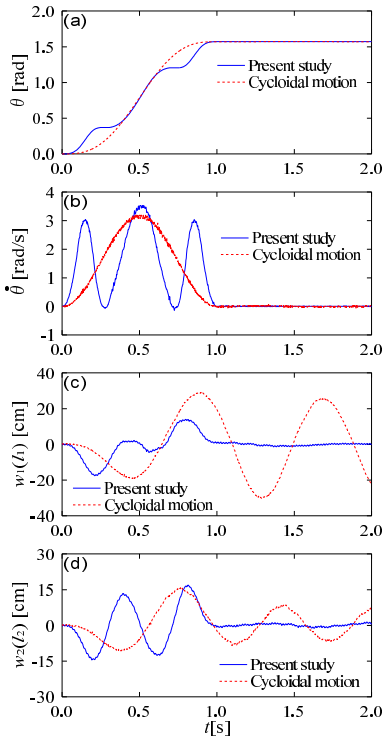

Fig. 8. Comparison of experimental results obtained by the present method and cycloidal motion ($T_E = 1.0$ s, $\theta_E = \pi/2$ rad): (a) joint angle, (b) angular velocity, (c) tip displacement of flexible link 1, and (d) tip displacement of flexible link 2.

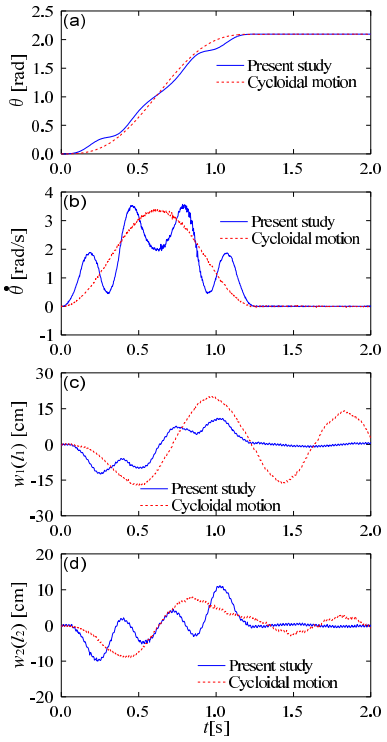

Fig. 9. Comparison of experimental results obtained by the present method and cycloidal motion ($T_E = 1.25$ s, $\theta_E = 2\pi/3$ rad): (a) joint angle, (b) angular velocity, (c) tip displacement of flexible link 1, and (d) tip displacement of flexible link 2.

along the optimal trajectory generated by the cubic spline function, the residual vibrations were perfectly canceled in comparison with the results obtained by a cycloidal motion. To demonstrate the feasibility of the proposed method, we also conducted experiments. From the experimental results, we concluded that the trajectory planning method developed in this study is effective and useful for the PTP motion of the flexible dual-manipulator. The proposed method requires exact mathematical models, and the robustness to parameter uncertainties has not been considered at present. However, the main feature of the proposed technique in which a cubic spline function and PSO are utilized, is that a feedforward controller can be constructed without the use of advanced control techniques.

REFERENCES

[1] M. Benosman and L. G. Vey, "Control of flexible manipulators: A survey," *Robotica*, vol. 22, no. 5, pp. 535–545, 2004.

[2] S. K. Dwivedy and P. Eberhard, "Dynamic analysis of flexible manipulators, A literature review," *Mechanism and Machine Theory*, vol. 41, no. 7, pp. 749–777, 2006.

[3] S. Yue, D. Henrich, W. L. Xu and S. K. Tso, "Point-to-point trajectory planning of flexible redundant robot manipulators using genetic algorithms," *Robotica*, vol. 20, no. 3, pp. 269–280, 2002.

[4] K. S. Lee and Y. S. Park, "Residual vibration reduction for a flexible structure using a modified input shaping technique," *Robotica*, vol. 20, no. 5, pp. 553–561, 2002.

[5] K. J. Park, "Path design of redundant flexible robot manipulators to reduce residual vibration in the presence of obstacles," *Robotica*, vol. 21, no. 3, pp. 335–340, 2003.

[6] K. J. Park, "Flexible robot manipulator path design to reduce the endpoint residual vibration under torque constraints," *Journal of Sound and Vibration*, vol. 275, no. 3/5, pp. 1051–1068, 2004.

[7] Z. Mohamed and M. O. Tokhi, "Command shaping techniques for vibration control of a flexible robot manipulator," *Mechatronics*, vol. 14, no. 1, pp. 69–90, 2004.

[8] V. Feliu, E. Pereira, I. M. Díaz and P. Roncero, "Feedforward control of multimode single-link flexible manipulators based on an optimal mechanical design," *Robotics and Autonomous Systems*, vol. 54, no. 8, pp. 651–666, 2006.

[9] H. Kojima and T. Hiruma, "Evolutionary learning acquisition of optimal joint angle trajectories of flexible robot arm," *Journal of Robotics and Mechatronics*, vol. 18, no. 1, pp. 103–110, 2006.

[10] M. S. Alam and M. O. Tokhi, "Designing feedforward command shapers with multi-objective genetic optimisation for vibration control of a single-link flexible manipulator," *Engineering Applications of Artificial Intelligence*, vol. 21, no. 2, pp. 229–246, 2008.

[11] I. M. Díaz, E. Pereira, V. Feliu and J. J. L. Cela, "Concurrent design of multimode input shapers and link dynamics for flexible manipulators," *IEEE/ASME Transactions on Mechatronics*, vol. 15, no. 4, pp. 646–651, 2010.

[12] A. Abe, "Trajectory planning for residual vibration suppression of a two-link rigid-flexible manipulator considering large deformation," *Mechanism and Machine Theory*, vol. 44, no. 9, pp. 1627–1639, 2009.

[13] A. Abe, "Trajectory planning for flexible Cartesian robot manipulator by using artificial neural network: Numerical simulation and experimental verification," *Robotica*, vol. 29, no. 5, pp. 797–804, 2011.

[14] J. Kennedy and R. C. Eberhart, "Particle swarm optimization", in *Proc. of the IEEE Int. Conf. on Neural Networks*, Perth, Washington, Vol.4, pp.1942–1948, 1995.

[15] M. Clerc and J. Kennedy, "The particle swarm-explosion, stability, and convergence in a multidimensional complex space," *IEEE Trans. Evolutionary Computation*, vol. 6, no. 1, pp. 58–73, 2002.

[16] H. Wu, F. Sun, Z. Sun and L. Wu, "Optimal trajectory planning of a flexible dual-arm space robot with vibration reduction," *Journal of Intelligent & Robotic Systems*, vol. 40, no. 2, pp. 147–163, 2004.